provides experimental support for LCAO-MO calculations, which place this valence σ ionization in close proximity to the π ionization. The complete interpretation of this state has important implications for the understanding of metal-metal interactions. An important factor contributing to the energy of the valence σ ionization appears to be direct interaction between the valence σ orbital density ($5d_{z^2}$) on one metal and the "core" (5s, $5p_z$) density on the neighboring metal atom.

Acknowledgments. We thank the Nationl Science Foundation (Grant No. CHE82-06117 to R.A.W. and CHE82-06169 to A.P.S.) and the Department of Energy (Contract No. DE-AC02-80ER10746 to D.L.L.) for support of this work. We appreciate the assistance of Stephen M. Tetrick in the measurement and interpretation of the NMR spectra, Arlene Rothwell for obtaining the EI and CI mass spectra, and Ann Copenhaver for analyzing the PE data.

Electronic and Vibrational Spectroscopy of the Triply Metal-Metal Bonded $Mo_2(HPO_4)_4^{2-}$ Ion. Inferences as to the Energetics of δ-Bonding from Spectroscopic Correlations to $Mo_2(SO_4)_4^{4-/3-}$

Michael D. Hopkins, Vincent M. Miskowski,* and Harry B. Gray*

Contribution No. 7273 from the Arthur Amos Noyes Laboratory, California Institute of Technology, Pasadena, California 91125. *Received August 26, 1985*

Abstract: Room- and low-temperature polarized single-crystal absorption spectra are reported for the triply metal-metal bonded $(pyH)_3[Mo_2(HPO_4)_4]Cl$ complex between 300 and 800 nm, and spectra to both higher and lower energy than this wavelength range are reported for a low-temperature pellet of $Cs_2[Mo_2(HPO_4)_4]\cdot 2H_2O$. Absorptions at 420, 542, and 670 nm in the single-crystal spectrum are assigned on the basis of their polarization and temperature behavior, as well as by comparison to previously unassigned bands in the spectra of $K_3[Mo_2(SO_4)_4]\cdot 3.5H_2O$ and $K_4[Mo_2(SO_4)_4]\cdot 2H_2O$, to $^1(\pi \rightarrow \delta^*)$, $^1(\pi \rightarrow \delta)$, and $^3(\pi \rightarrow \delta)$, respectively. A band at 340 nm, which is not observed in the pellet spectrum of the Cs^+ salt or in solution, is assigned to $\sigma(Mo\text{-}Cl) \rightarrow \delta(Mo_2)$ LMCT, while an intense absorption at 250 nm in the pellet spectrum is tentatively attributed to the $^1(\pi \rightarrow \pi^*)(Mo_2)$ transition. A Faraday magnetic measurement supports the proposed $(\sigma^2\pi^4)$ triple-bond ground state of $Mo_2(HPO_4)_4^{2-}$, which displays the Raman-active $\nu(Mo_2)$ vibration at $\sim$360 cm^{-1} for both salts. The differences in observed metal-metal stretching frequencies and the observed and calculated one-electron splitting of the δ and δ^* levels of the Mo_2(III,III) phosphate and Mo_2(II,III) and Mo_2(II,II) sulfate complexes are entirely consistent with the change in formal metal-metal bond order from 3 to 4 across this series.

Spectroscopic studies of the $^1(\delta \rightarrow \delta^*)$ transition of quadruply bonded metal dimers have been of central importance in elucidating the electronic structural details of the δ-bond present in this class of compounds.[1,2] One of the principal themes that has emerged from consideration of the overall spectral behavior of these systems is that the relatively high energy and low intensity of this transition are a direct consequence of the weak overlap of the d_{xy} orbitals that comprise the δ-interaction.[1] The actual contribution of the energetic splitting of the one-electron δ and δ^* levels to the energy of the $^1(\delta\delta^*)$ state, however, has been difficult to assess experimentally,[3-5] and hence quantitative spectroscopic measurements of the extent to which the δ-interaction is perturbed by such variables as metal-metal distance, metal-ligand interactions, and formal charge of the M_2 unit have, for the most part, remained elusive.

Binuclear complexes that span a wide range of d-electron counts and formal metal-metal bond orders have been prepared and structurally characterized, particularly over the last 25 years.[2] Several years ago, compounds containing the $Mo_2(SO_4)_4^{4-/3-}$ ions, which constitute examples of bond orders of $4(\sigma^2\pi^4\delta^2)$ and 3.5-$(\sigma^2\pi^4\delta^1)$, respectively, were reported[6] and subsequently thoroughly characterized with respect to their spectroscopic properties.[7-11] This series has recently been extended to include an example with a formal bond order of 3 with the discovery of the structurally related $Mo_2(HPO_4)_4^{2-}$ ion,[12,13] which is proposed to possess a $(\sigma^2\pi^4\delta^0)$ electronic configuration. Comparisons of the molecular structures of these three compounds show that the major perturbation to the Mo_2O_8 core across this series is a small, monotonic increase in the metal-metal distance with decreasing bond order ($\sim$0.06 Å/δ electron),[12] as anticipated from qualitative electronic structural considerations. We report herein the results of our electronic and vibrational spectroscopic investigation of the $Mo_2(HPO_4)_4^{2-}$ ion, as well as the correlation of the relative energies of the π, δ, and δ^* levels with metal oxidation state and metal-metal distance for this class of complexes.

Experimental Section

General Procedures. All chemicals were of reagent grade or comparable quality and were used as received. Elemental analyses were performed by Mr. Larry Henling at the Caltech Analytical Laboratory. Magnetic susceptibilities were obtained at room temperature with a Faraday balance that was calibrated with $HgCo(SCN)_4$. Raman spectra

---

[1] Trogler, W. C.; Gray, H. B. *Acc. Chem. Res.* **1978**, *11*, 232-239.

[2] Cotton, F. A.; Walton, R. A. "Multiple Bonds Between Metal Atoms"; Wiley: New York, 1982.

[3] Hopkins, M. D.; Zietlow, T. C.; Miskowski, V. M.; Gray, H. B. *J. Am. Chem. Soc.* **1985**, *107*, 510-512.

[4] Campbell, F. L., III; Cotton, F. A.; Powell, G. L. *Inorg. Chem.* **1985**, *24*, 177-181.

[5] Manning, M. C.; Trogler, W. C. *J. Am. Chem. Soc.* **1983**, *105*, 5311-5320.

[6] Bowen, A. R.; Taube, H. *J. Am. Chem. Soc.* **1971**, *93*, 3287-3289. Bowen, A. R.; Taube, H. *Inorg. Chem.* **1974**, *13*, 2245-2249. Cotton, F. A.; Frenz, B. A.; Pedersen, E.; Webb, T. R. *Inorg. Chem.* **1975**, *14*, 391-398.

[7] Angell, C. L.; Cotton, F. A.; Frenz, B. A.; Webb, T. R. *J. Chem. Soc., Chem. Commun.* **1973**, 399-400.

[8] Loewenschuss, A.; Shamir, J.; Ardon, M. *Inorg. Chem.* **1976**, *15*, 238-241.

[9] Cotton, F. A.; Martin, D. S.; Fanwick, P. E.; Peters, T. J.; Webb, T. R. *J. Am. Chem. Soc.* **1976**, *98*, 4681-4682.

[10] Erwin, D. K.; Geoffroy, G. L.; Gray, H. B.; Hammond, G. S.; Solomon, E. I.; Trogler, W. C.; Zagars, A. A. *J. Am. Chem. Soc.* **1977**, *99*, 3620-3621.

[11] Fanwick, P. E.; Martin, D. S.; Webb, T. R.; Robbins, G. A.; Newman, R. A. *Inorg. Chem.* **1978**, *17*, 2723-2727.

[12] Bino, A.; Cotton, F. A. *Angew. Chem., Int. Ed. Engl.* **1979**, *18*, 462-463. Bino, A.; Cotton, F. A. *Inorg. Chem.* **1979**, *18*, 3562-3565.

[13] Bino, A. *Inorg. Chem.* **1981**, *20*, 623-626.

0002-7863/86/1508-0959$01.50/0

were recorded on a Spex Ramalog EU spectrometer equipped with a cooled RCA 31034A photomultiplier tube, an ORTEC 9300 series photon counter, and a Nicolet 1180E Raman data system. Absorption spectra were recorded with a Cary 17 spectrophotometer; spectra at low temperature were obtained with either a Cryogenic Technologies Model 21 closed-cycle helium refrigerator (18K measurements) or an Oxford Instruments Model CF-204 continuous-flow cryostat (4.2K measurements). Polarized single-crystal experiments were performed on crystals mounted on quartz flats, the area around the crystal being carefully masked with heat-conducting grease. Polarized light was obtained with dual Glan-Thompson air-spaced calcite polarizers.

$(pyH)_3[Mo_2(HPO_4)_4]Cl$.[14] A saturated solution of $K_4Mo_2Cl_8$ in N_2-purged 6 N H_3PO_4 was quickly filtered, in air, into an open beaker containing a 5-fold excess of pyridinium chloride. The solution became turbid shortly after dissolution of the salt, and within minutes a gray precipitate had formed. After being stirred for 10 min, the mixture was diluted by 25% with 6 N H_3PO_4, stirred briefly, and filtered. The filtrate was again diluted by 25% with 6 N H_3PO_4, and the deep yellow solution was allowed to stand undisturbed in an open beaker. After 24 h, several fine purple needles were observed to be growing on the wall of the beaker at the solvent/air interface, in addition to a small amount of gray precipitate on the bottom of the beaker. After 3 days, a small crop (10–20 crystals) of long (1–1.5 cm) red-purple blades was carefully removed from the flask and blotted dry between sheets of filter paper. Additional material could be obtained as small red-purple needles by allowing the combined gray precipitates to stand in the mother liquor in an open beaker for 1 month. This material was washed with a small amount of ethanol and dried in vacuo. Anal. Calcd (found) for $C_{15}H_{22}N_3ClO_{16}P_4Mo_2$: C, 21.16 (21.10); H, 2.60 (2.56); N, 4.93 (4.91).

Examination of the blade-like crystals under a polarizing microscope revealed sharp extinctions parallel and perpendicular to the blade axis. Most of these crystals were aggregates that were aligned along the blade axis. Small, thin single crystals could be obtained by breaking up these aggregates; all spectral data in this paper refer to such crystals. These crystals were strongly dichroic, transmitting yellow and red-purple light for their parallel and perpendicular extinctions, respectively. Examination of a typical crystal by X-ray photographic methods showed it to be consistent with the previously reported[12] orthorhombic space group (*Pbam*) and lattice constants. The crystallographic *c* axis was found to be colinear with the long blade axis (yellow extinction) of the crystal, and the well-developed crystal face was determined to be (100). The yellow and reddish-purple extinction directions therefore correspond to polarization parallel and perpendicular, respectively, to the linear $-(Mo-Mo-Cl-)_\infty$ chains (C_{2h} site symmetry) of the crystal, i.e., respectively parallel and perpendicular to molecular *z*.

$Cs_2[Mo_2(HPO_4)_4]\cdot 2H_2O$. A 50% saturation solution of $(pyH)_3[Mo_2(HPO_4)_4]Cl$ in N_2-purged 6 N H_3PO_4 was treated dropwise with a saturated solution of CsCl in the same solvent. The product precipitated immediately, as a fine purple powder, in nearly quantitative yield.

Results and Discussion

Magnetism. Although the $(\sigma^2\pi^4\delta^0)$ electronic configuration proposed[12,13] for $Mo_2(HPO_4)_4^{2-}$ seemed very likely to be correct, a recent report of paramagnetism for the $Os_2(O_2CR)_4Cl_2$ compounds,[15] which possess two electrons in excess of a quadruple bond, made magnetic confirmation of the singlet ground state desirable. A room temperature (297 K) Faraday measurement on our preparation of $(pyH)_3[Mo_2(HPO_4)_4]Cl$ showed it to be rigorously diamagnetic, in accord with previous predictions, with the observed susceptibility of $\chi_m = -100(10) \times 10^{-6}$ emu/mol being in fair agreement with that calculated by standard methods[16] $(-350 \times 10^{-6}$ emu/mol).

Raman Spectroscopy. The Raman spectra obtained for $(pyH)_3[Mo_2(HPO_4)_4]Cl$ and $Cs_2[Mo_2(HPO_4)_4]\cdot 2H_2O$ upon 363.8-nm excitation are reproduced in Figure 1.[17] The strongest feature in each spectrum is a line at ~360 cm^{-1} that is readily assigned to $\nu(Mo_2)$ by analogy to the previously reported metal–metal stretching frequencies of $Mo_2(SO_4)_4^{4-}$ (371 cm^{-1})[7,8] and $Mo_2(SO_4)_4^{3-}$ (373, 386 cm^{-1})[8] (the dual frequencies observed for the latter ion are a consequence of the existence of two crystallographically distinct dimers in the unit cell). Although the trend of $\nu(Mo_2)$ among the Mo_2(II,II) and Mo_2(II,III) sulfates is not an obvious one, the frequency of the Mo_2(III,III) phosphate is clearly lower than both of them, in accord with its lower bond order and longer metal–metal bond. Additional evidence that this is a reasonable assignment for $\nu(Mo_2)$ comes from comparison with the $^2(\delta \rightarrow \delta^*)$ excited state of the Mo_2(II,III) sulfate,[10,11] which has a formal bond order of $2.5(\sigma^2\pi^4\delta^{*1})$ and a concomitantly lower metal–metal stretching frequency $\nu(Mo_2) = 350$ cm^{-1}.[18]

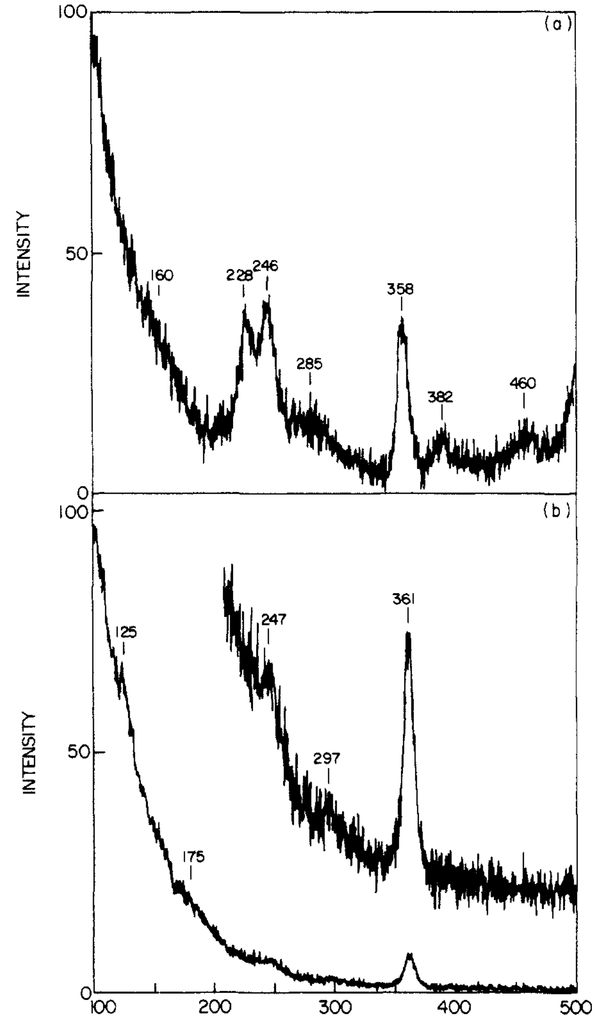

Figure 1. Raman spectra of (a) $Cs_2[Mo_2(HPO_4)_4]\cdot 2H_2O$ and (b) $(pyH)_3[Mo_2(HPO_4)_4]Cl$ (λ_{ex} = 363.8 nm) at room temperature.

With respect to the frequencies of metal–ligand vibrations, each Raman spectrum shows well-defined lines between 200 and 300 cm^{-1}; analogous lines observed for the Mo_2 sulfates have been assigned[8] to ν(Mo–O(sulfate)) modes. These assignments seem reasonable, although deformation modes (δ(Mo–O)) are also candidates for the lines in this region.[19] The pyH^+ salt should, in addition, possess a feature attributable to the ν(Mo–Cl) mode, although the extreme length of this bond (2.91 Å)[12] suggests that it must lie at relatively low frequency. The shoulder at 125 cm^{-1}, which has no counterpart in the Cs^+ spectrum, seems reasonable

---

(14) This revision of the original synthesis[12] was worked out in consultation with Dr. A. Bino with the aim of obtaining material suitable for single-crystal absorption spectroscopy.

(15) Behling, T.; Wilkinson, G.; Stephenson, T. A.; Tocher, D. A. *J. Chem. Soc., Dalton Trans.* **1983**, 2109–2116.

(16) Earnshaw, A. "Introduction to Magnetochemistry"; Academic Press: New York, 1968.

(17) We obtained Raman spectra using UV (363.8 nm) excitation with the aim of achieving preresonance enhancement with UV electronic absorption bands (e.g., $\pi \rightarrow \pi^*$, LMCT: vide infra) that are much more intense than those observed in the visible region. Raman scattering by these solids is indeed stronger for UV excitation, and some selective enhancement of $\nu(Mo_2)$ is observed.

(18) With regard to the metal–metal stretching frequencies of the Mo_2(II,II) and Mo_2(II,III) sulfates, assuming $r(M_2) \propto [k(M_2)]^{-1/3}$ (cf. Badger's rule) using Mo_2(III,III) phosphate as a benchmark (k = 3.7 mdyne/Å; M_2 approximation) leads to calculated values of ~390 and 375 cm^{-1} for the bond order 4 and 3.5 cases, respectively. Similar application to the $^2(\delta \rightarrow \delta^*)$ excited state of Mo_2(II,III) sulfate yields a bond lengthening of ~0.04 Å on the change from bond order 3 to 2.5.

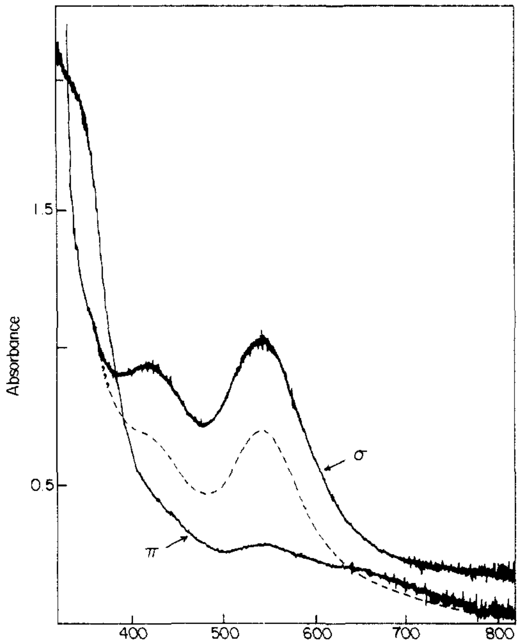

Figure 2. Polarized single-crystal absorption spectrum of $(pyH)_3[Mo_2(HPO_4)_4]Cl$ at room temperature. The σ spectrum is vertically offset from the π spectrum by 0.15 optical density units. The dashed line is the calculated isotropic spectrum, $\epsilon(\text{isotropic}) = {}^1/_3(\epsilon_\pi + 2\epsilon_\sigma)$, with the π base line.

in this regard. Additional weak features observed below 200 cm^{-1} remain unassigned; δ(Mo–O) deformation modes undoubtedly contribute to this region of the spectrum.[8,19]

Finally, lines to higher frequency of $\nu(Mo_2)$ are presumably associated with vibrations of the phosphate moiety; "free" PO_4^{3-} has modes at 420 and 567 cm^{-1},[20] and the sulfate complexes again show analogous lines.[8]

Electronic Spectroscopy. Electronic absorption spectra have been reported in the visible region for solutions of $Mo_2(HPO_4)_4^{2-}$,[13] as well as for a KBr pellet of the Cs^+ salt,[12] at room temperature. The two spectra are virtually identical, consisting of weak bands at λ_{max} 428 nm ($\epsilon = 63\ M^{-1}\ cm^{-1}$) and λ_{max} 548 (ϵ 107).[13] We have examined a dilute CsCl pellet of $Cs_2[Mo_2(HPO_4)_4]\cdot 2H_2O$ at 5 K and found an additional, relatively intense absorption centered at 250 nm. Neither this feature nor the previously reported visible bands displayed vibronic stucture at low temperature, however.

The polarized single-crystal absorption spectra of $(pyH)_3[Mo_2(HPO_4)_4]Cl$ at room and low temperature are displayed in Figures 2 and 3, respectively.[21] These spectra show strongly $\sigma(x,y)$-polarized bands with nearly temperature-independent maxima at 542 and 420 nm, and which are clearly analogous to those observed in solution. The integrated intensity of each band in $\pi(z)$-polarization decreases with decreasing temperature, indicating that it is vibronically induced. The oscillator strength of the 542-nm band in x,y-polarization is independent of temperature, suggesting that this transition is dipole-allowed. In contrast, the 420-nm band in this polarization is less well defined at low temperatures, indicating that it is losing intensity and is thus likely to be dipole-forbidden in x,y- as well as z-polarization. The fact that this band is located on the low-energy tail of a much more intense transition makes our conclusions for the 420-nm band less certain than for the 542-nm band, however.

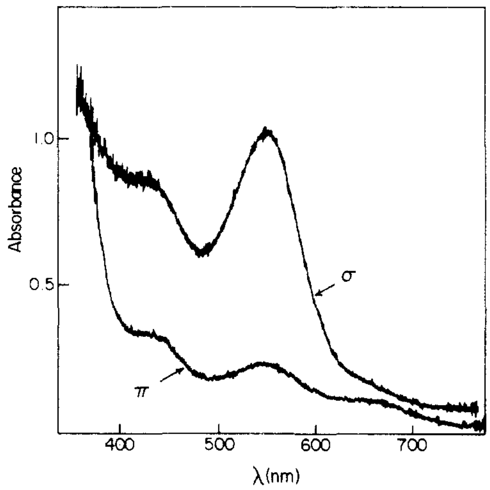

Figure 3. Polarized single-crystal absorption spectrum of $(pyH)_3[Mo_2(HPO_4)_4]Cl$ at 18 K. The σ spectrum is vertically offset from the π spectrum by 0.06 optical density units.

In addition to the two transitions that have analogues in the solution spectrum of $Mo_2(HPO_4)_4^{2-}$, two previously unreported bands were observed in the single-crystal spectra. The first is a broad, weak feature at ~670 nm that is predominantly z-polarized, although a weak shoulder in x,y-polarization at roughly the same wavelength is evident at low temperature. At room temperature, this band contributes only to the long-wavelength tail in the calculated isotropic absorption spectrum (Figure 2). Since a similar tail is seen in both the solution[13] and pellet spectra,[12] we consider the 670-nm band to be an authentic absorption of the $Mo_2(HPO_4)_4^{2-}$ chromophore. The second previously unreported band of $(pyH)_3[Mo_2(HPO_4)_4]Cl$ is a predominantly z-polarized absorption centered at 340 nm that, in contrast, has *no* counterpart in either the pellet spectrum of $Cs_2[Mo_2(HPO_4)_4]\cdot 2H_2O$ or in solution spectra,[13] and which accounts for the visibly more reddish-purple color of the pyH^+ salt relative to the pure purple color of the Cs^+ adduct. We infer from the fact the 340-nm absorption is unique to the pyH^+ compound that this band is not metal–metal-localized, and suggest that it is attributable to an LMCT transition involving the infinite-chain-bridging axial chloride ligands present in this particular salt. The extreme length of the Mo–Cl bonds could conceivably account for the relative weakness of this transition. A calculation by Norman et al.[22] on the $(\sigma^2\pi^4\delta^2\pi^{*2}\delta^{*1})$ ground state of the structurally related $Ru_2(O_2CH)_4Cl_2^-$ ions assigns the highest occupied halide level to be a_{1g} σ(Ru–Cl), located at slightly higher energy than $\delta(Ru_2)$. The most likely assignment of the observed band is therefore $\sigma(\text{Mo–Cl}) \rightarrow \delta(Mo_2)$, which is dipole-forbidden. Unfortunately, we were unable to extend our low-temperature measurements to sufficiently high optical density to test the implied temperature-dependent intensity of this assignment.

Assignment of the Metal–Metal Transitions. The absorption bands of $(pyH)_3[Mo_2(HPO_4)_4]Cl$ at 542 and 420 nm, and probably also that at 670 nm, are likely to be electronic transitions associated with its metal–metal bonding framework. In deriving assignments for these bands, we draw heavily upon comparisons to the data accumulated by Martin and co-workers for the Mo_2(II,II)[9] and Mo_2(II,III)[11] sulfate complexes. We assume that the bridging HPO_4^{2-} and SO_4^{2-} ligands are very similar from an electronic standpoint, and such comparisons as are available[6,12,13,23] support this contention.

The metal–metal-localized electronic transitions between the π- and δ-based manifold of states of $Mo_2(HPO_4)_4^{2-}$ and Mo_2-

---

(19) Bratton, W. K.; Cotton, F. A.; DeBeau, M.; Walton, R. A. *J. Coord. Chem.* **1971**, *1*, 121–131.

(20) Nakamoto, K. "Infrared and Raman Spectra of Inorganic and Coordination Compounds"; Wiley: New York, 1978; p 142.

(21) Neither the crystal spectra of the pyH^+ salt nor the pellet spectrum of the Cs^+ salt displayed electronic absorptions in the near-infrared. In addition to demonstrating the absence of intrinsic electronic transitions in this region, this result rules out the possibility of contamination of these materials with $Mo_2(HPO_4)_4^{3-}$ ions,[13] which should display a $\delta \rightarrow \delta^*$ absorption below 1000 nm.[10,11]

(22) Norman, J. G., Jr.; Renzoni, G. E.; Case, D. A. *J. Am. Chem. Soc.* **1979**, *101*, 5256–5267.

(23) Pt_2(III,III) sulfate/phosphate complexes: Orlova, V. S.; Muraveiskaya, G. S.; Evstaf'eva, O. N. *Russ. J. Inorg. Chem.* **1975**, *20*, 753–758. Bancroft, D. P.; Cotton, F. A.; Falvello, L. R.; Han, S.; Schwotzer, W. *Inorg. Chim. Acta* **1984**, *87*, 147–153.

Table I. Spin-Allowed Electronic Transitions Involving the π, δ, δ^*, and π^* Levels of $Mo_2(SO_4)_4^{4-/3-}$ and $Mo_2(HPO_4)_4^{2-}$ [a]

	assignment (position/nm)			
orbital transition	Mo_2(II,II) $\leftarrow {}^1A_{1g}$	Mo_2(II,III) $\leftarrow {}^2B_{2g}$	Mo_2(III,III) $\leftarrow {}^1A_{1g}$	electric dipole polarization
$\pi(e_u) \rightarrow \delta(b_{2g})$	*b*	${}^2E_u$(595)	${}^1E_u$(542)	*x*, *y*
$\pi(e_u) \rightarrow \delta^*(b_{1u})$	${}^1E_g$(400)	${}^2E_g$(417)	${}^1E_g$(420)	dipole-forbidden
$\pi(e_u) \rightarrow \pi^*(e_g)$	*c*	*c*	${}^1A_{2u}$(250?)	*z*
$\delta(b_{2g}) \rightarrow \delta^*(b_{1u})$	${}^1A_{2u}$(515)	${}^2B_{1u}$(1400)	*b*	*z*
$\delta(b_{2g}) \rightarrow \pi^*(e_g)$	*c*	*c*	*b*	dipole-forbidden

[a] D_{4h} molecular symmetry. [b] Transition does not occur in this species. [c] Not assigned.

$(SO_4)_4^{4-/3-}$ are set out in Table I. For the Mo_2(II,II) sulfate complex, which has a $(\sigma^2\pi^4\delta^2)$ ground state, crystal spectra of the K^+ salt show[9] the lowest energy transition to be the strongly *z*-polarized, moderately intense (ϵ_{max} 170 in solution)[10] ${}^1(\delta \rightarrow \delta^*)$ absorption at 515 nm. The one-electron-oxidized, $(\sigma^2\pi^4\delta^1)$-configured Mo_2(II,III) sulfate displays[11] as its lowest transition the similarly intense,[10] *z*-polarized ${}^2(\delta \rightarrow \delta^*)$ band centered at 1400 nm, the large red shift being understandable in terms of the large contribution of two-electron terms to the energy of the singlet transition.[3,4] The $(\sigma^2\pi^4)$ Mo_2(III,III) phosphate cannot, of course, have a $\delta \rightarrow \delta^*$ absorption, and thus its lowest energy allowed transitions are likely to be $\pi \rightarrow \delta$ and $\pi \rightarrow \delta^*$ (Table I). Both of these transitions should also be present in the Mo_2(II,III) sulfate, while the Mo_2(II,II) sulfate can possess only the $\pi \rightarrow \delta^*$ band.

The single-crystal absorption spectrum of $Mo_2(SO_4)_4^{3-}$ showed, in addition to ${}^2(\delta \rightarrow \delta^*)$, weak bands at 595 nm (*x*,*y*-polarized, temperature-independent intensity) and 417 nm (indefinite polarization and thermal behavior). These compare quite closely in energy and behavior to the 542- and 420-nm absorptions observed by us for $Mo_2(HPO_4)_4^{2-}$, and we suggest that these bands may be assigned to the $\pi \rightarrow \delta$ and $\pi \rightarrow \delta^*$ transitions, respectively. The spectrum of $Mo_2(SO_4)_4^{4-}$ also contains a weak band of mixed polarization at 400 nm which, by analogy to the 417- and 420-nm bands of Mo_2(II,III) and Mo_2(III,III) systems, respectively, could be attributable to the $\pi \rightarrow \delta^*$ transition.

Martin and co-workers considered a $\pi \rightarrow \delta$ $({}^2E_u \leftarrow {}^2B_{2g})$ assignment for the visible absorptions of the Mo_2(II,III) sulfate, but they argued that the intensities of these bands were too low for dipole-allowed transitions. In view of the similarly small oscillator strengths of the dipole-allowed $\delta \rightarrow \delta^*$ transitions of the sulfate compounds, however, we suggest that the observed intensities are actually quite reasonable. Moreover, there is one very satisfying aspect of our assignments. The *difference* of the energies of the $\pi \rightarrow \delta$ and $\pi \rightarrow \delta^*$ transitions should equal the one-electron orbital splitting of the δ and δ^* levels; the above assignments of these bands yield a δ–δ^* splitting of 7175 cm^{-1}, in essentially perfect agreement with the directly observed 7150-cm^{-1} energy[10,11] of the ${}^2(\delta \rightarrow \delta^*)$ transition of this complex.[24]

Application of this analysis to the Mo_2(III,III) phosphate yields a δ–δ^* orbital splitting of 5100 cm^{-1},[25] reduced, as expected, as a result of the longer bond distance and lower bond order of this complex.[26] By assuming that the average energy of the δ and δ^* levels remains constant for the bond order 3 and 3.5 complexes, then our assignments yield the energy level diagram shown in Figure 4. One consequence of this assumption is that the energy of the π level is nearly independent of the differences between the bond orders and metal–metal distances of these two compounds. Inasmuch as the δ-interaction is significantly weaker than the π-interaction in these complexes, the former's sensitivity to bond order and bond distance should be dramatically more marked than the latter's. By additionally assuming that the constant energy of the π level extends to the bond-order 4 case, then our assignment of the $\pi \rightarrow \delta^*$ transition of Mo_2(II,II) sulfate allows us to infer a one-electron δ–δ^* splitting of ~8500 cm^{-1} for the quadruple bond, which is in reasonable agreement with the results of calculations[27] on other Mo_2(II,II) complexes possessing similar ${}^1(\delta \rightarrow \delta^*)$ transition energies.[28]

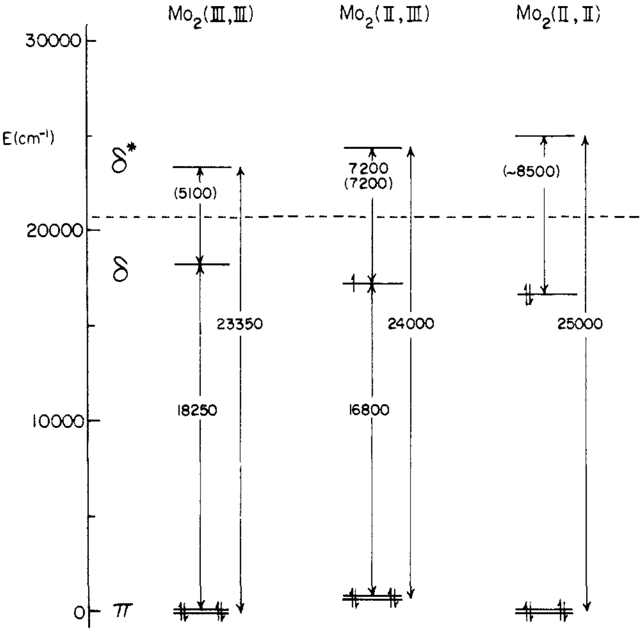

Figure 4. Energies of the π, δ, and δ^* levels of $Mo_2(HPO_4)_4^{2-}$, $Mo_2(SO_4)_4^{3-}$, and $Mo_2(SO_4)_4^{4-}$. Calculated or estimated energies are given in parentheses; all other values are spectroscopically determined.

We also wish to consider briefly the assignments of the two other bands observed in the solid-state spectra of $Mo_2(HPO_4)_4^{2-}$. The weak, predominantly *z*-polarized feature at ~670 nm in the single-crystal spectra of $(pyH)_3[Mo_2(HPO_4)_4]Cl$ is attributable to the ${}^3(\pi \rightarrow \delta)$ $({}^3E_u \leftarrow {}^1A_{1g})$ excitation, which should possess both *z*- and *x*,*y*-allowed components. The intensity of this band relative to its singlet counterpart, as well as the resulting singlet–triplet splitting (~3500 cm^{-1}), are in reasonable agreement with ex-

---

(24) The Mo_2(II,II) and Mo_2(II,III) sulfate complexes should also have a $\delta \rightarrow \pi^*$ transition that is absent in the Mo_2(III,III) phosphate. The close coincidence of the visible absorption bands for the latter two complexes, as well as the reproduction of the ${}^2(\delta \rightarrow \delta^*)$ transition energy by this calculation, makes assignment of either the 417- or 595-nm band of $Mo_2(SO_4)_4^{3-}$ to $\delta \rightarrow \pi^*$ far less satisfactory than those proposed here. The spectra of the sulfate complexes contain[9,11] additional weak bands between 300 and 350 nm for which a $\delta \rightarrow \pi^*$ assignment is possible.

(25) Since the actual peak position of the 420-nm band of $Mo_2(HPO_4)_4^{2-}$ is not well determined in our single-crystal spectra, we used the 428- and 548-nm values taken from solution.[13] Vertical transition energies were used in all instances.

(26) In extending this analysis to $Mo_2(HPO_4)_4^{2-}$ we are assuming that the contributions to interconfigurational transitions (e.g., $\pi \rightarrow \delta^*$) from two-electron terms will roughly cancel out when the differences between these transition energies are taken, thus yielding one-electron orbital splittings of the type directly measured in the spectrum of $Mo_2(SO_4)_4^{3-}$. Such an approximation cannot, of course, be applied to transitions between covalent and ionic states (e.g., ${}^1(\delta \rightarrow \delta^*)$).[3,4]

(27) $Mo_2Cl_8^{4-}$: $E(\delta^*-\delta) = 7900$ cm^{-1} (Norman, J. G., Jr.; Ryan, P. B. *J. Comput. Chem.* **1980**, *1*, 59–63). $Mo_2Cl_4(PMe_3)_4$: $E(\delta^*-\delta) = 8070$ cm^{-1} (Cotton, F. A.; Hubbard, J. L.; Lichtenberger, D. L.; Shim, I. *J. Am. Chem. Soc.* **1982**, *104*, 679–686).

(28) Analogous studies have been reported for $Re_2Cl_4(PR_3)_4^{2+/+/0}$ $(\sigma^2\pi^4\delta^2\delta^{*n}$, $n = 0, 1, 2)$. (Bursten, B. E.; Cotton, F. A.; Fanwick, P. E.; Stanley, G. G.; Walton, R. A. *J. Am. Chem. Soc.* **1983**, *105*, 2606–2611. Cotton, F. A.; Dunbar, K. R.; Falvello, L. R.; Tomas, M.; Walton, R. A. *Ibid.* **1983**, *105*, 4950–4954). Extensive mixing between metal- and ligand-based levels of these systems, and concomitantly lower energy LMCT transitions, precluded a spectroscopic analysis as straightforward as that presented here for the Mo_2 sulfate/phosphate complexes, for which such complications are likely to be minimal.

pectations for a second-row transition-metal complex.[29] Finally, our pellet spectrum of $Cs_2[Mo_2(HPO_4)_4]\cdot 2H_2O$ showed a very intense absorption maximum at 250 nm. We consider it most unlikely that intense charge-transfer transitions involving the bridging phosphate or axial water ligands would occur at this low an energy and thus tentatively suggest that this band be assigned to the $^1(\pi \rightarrow \pi^*)(Mo_2)$ transition. Comparable UV data for the analogous sulfate complexes, however, have not yet been reported.

Acknowledgment. We thank W. H. Woodruff and W. P. Schaefer for assistance with the Raman spectroscopy and X-ray photography, respectively, and A. Bino for helpful discussions regarding the preparation of $Mo_2(HPO_4)_4^{2-}$. M.D.H. acknowledges the Sun Co. and Standard Oil Co. (Ohio) for graduate fellowships. This work was supported by National Science Foundation Grant CHE84-19828 (H.B.G.) and the Caltech President's Fund (V.M.M.).

Registry No. $(pyH)_3[Mo_2(HPO_4)_4]Cl$, 71597-13-2; $Cs_2[Mo_2(HPO_4)_4]\cdot 2H_2O$, 70281-26-4; $Mo_2(SO_4)_4^{4-}$, 63313-38-2; $Mo_2(HPO_4)_4^{2-}$, 75365-59-2.

---

[29] An alternative assignment for the 670-nm band is $^1(\sigma(Mo_2) \rightarrow \delta\text{-}(Mo_2))$ ($^1B_{2g} \leftarrow {}^1A_{1g}$; dipole-forbidden); recent photoelectron spectroscopic studies of other triply metal–metal bonded complexes indicate that the σ and π molecular orbitals of these species are nearly degenerate (Kober, E. M.; Lichtenberger, D. L. *J. Am. Chem. Soc.* **1985**, *107*, 7199–7201).

Mixed-Valence 1′,6′-Dihalobiferrocenium Salts: The Effect of the Solid-State Environment on Electron-Transfer Rates

Teng-Yuan Dong,[1] David N. Hendrickson,*[1] Cortlandt G. Pierpont,*[2] and Michael F. Moore[1]

Contribution from the School of Chemical Sciences, University of Illinois, Urbana, Illinois 61801, and the Department of Chemistry, University of Colorado, Boulder, Colorado 80309. *Received July 23, 1985*

Abstract: Results for the room-temperature X-ray structures of mixed-valence 1′,6′-diiodobiferrocenium triiodide (**2**) and mixed-valence 1′,6′-dichlorobiferrocenium octaiodide(2−) (**4**) are reported. An interesting observation was made: the mixed-valence cation in **4** is valence localized with Fe^{II} and Fe^{III} ions, whereas, the cation in **2** has two crystallographically equivalent iron ions. In the case of **2** the structure was refined to give discrepancy factors of $R_F = 0.033$ and $R_{wF} = 0.038$ for 946 observed ($|F| > 6\sigma|F|$) reflections. Compound **2** crystallizes in the monoclinic space group $C2/m$ with two formula weights in a cell having the dimensions $a = 12.282$ (2) Å, $b = 8.935$ (1) Å, $c = 12.287$ (2) Å, and $\beta = 61.89$ (1)°. The mixed-valence 1′,6′-diiodobiferrocenium cation lies on a crystallographic mirror plane and is located about a twofold axis in the unit cell, imposing $2/m$ symmetry (trans conformation) on the cation. The packing arrangement in **2** consists of planar layers of cations and anions that are arranged in an alternating fashion on the crystallographic *ac* mirror plane. In the case of **4** the X-ray structure was refined to give discrepancy factors of $R_F = 0.064$ and $R_{wF} = 0.068$ for 1084 observed ($|F| > 6\sigma|F|$) reflections. Compound **4** crystallizes in the monoclinic space group $I2$ with four formula weights in a cell having the dimensions $a = 13.709$ (2) Å, $b = 14.189$ (2) Å, $c = 14.409$ (2) Å, and $\beta = 116.64$ (2)°. No crystallographic symmetry is imposed on the mixed-valence 1′,6′-dichlorobiferrocenium cation, although it does have the same trans conformation as found for the 1′,6′-diiodobiferrocenium cation. In marked contrast to the cation in **2**, for the 1′,6′-dichlorobiferrocenium cation one-half of the molecule has the dimensions of a Fe^{II} metallocene and the other half those of a Fe^{III} metallocene. In **4** the solid-state environments of the two iron ions in one cation are quite different due to the positioning of the I_3^- counterion, whereas, the anion in **2** is positioned symmetrically relative to the two iron ions in the cation. Variable-temperature ^{57}Fe Mössbauer, EPR, and IR data are presented for **2**, **4**, and 1′,6′-dibromobiferrocenium triiodide (**3**). Compound **4** gives a Mössbauer spectrum with two quadrupole-split doublets at 4.2 K; two doublets are also seen in the 340 K spectrum. On the other hand, compounds **2** and **3** give Mössbauer spectra with a single "average-valence" quadrupole-split doublet at 300 K. Furthermore, a single doublet is seen at 4.2 K for **2** and **3**. Compounds **2** and **3** exhibit relatively isotropic **g** tensors compared to **4**, as deduced from X-band EPR spectra. Compounds **2** and **3** are judged to have an intramolecular electron-transfer rate in excess of the Mössbauer and EPR time scales (rate $> \sim 10^{10}$ s^{-1}), whereas, the electron-transfer rate for **4** is slower than $\sim 10^7$ s^{-1}. However, all three compounds are found to be localized on the infrared time scale. It is concluded that it is *not* a variation in the electronic coupling between iron ions nor the vibronic coupling that leads to the appreciable change in electron-transfer rate that occurs in going from the dichloro cation to the two others. The differences in rates are attributable to differences in the symmetry of the solid-state environment.

Recent results obtained for the mixed-valence biferrocenes **1**–**8** have given insight about the influence of the solid-state environment on the rate of intramolecular electron transfer. Very recently the X-ray structures of **1**[3,4] and **7**[4] were reported. Previously compound **1** had been reported[5] to be localized on the Mössbauer time scale at 300 K. However, recently it was found[3,4] that at temperatures above 300 K the ^{57}Fe Mössbauer spectrum of **1** changes from two doublets to eventually become a single average-valence doublet at ~357 K. Mixed-valence compounds **5**,[6] **6**,[6] **7**,[4] and **8**[4] were also found to have temperature-dependent Mössbauer spectra. At temperatures below ~200 K they each show two doublets, one for the Fe^{II} and the other for the Fe^{III} site. As the temperature of these four compounds is increased above ~200 K the two doublets move together to become a single

---

[1] University of Illinois.

[2] University of Colorado.

[3] Cohn, M. J.; Dong, T.-Y.; Hendrickson, D. N.; Geib, S. J.; Rheingold, A. L. *J. Chem. Soc., Chem. Commun.* **1985**, *1095*.

[4] Dong, T.-Y.; Hendrickson, D. N.; Iwai, K.; Cohn, M. J.; Rheingold, A. L.; Sano, H.; Motoyama, I.; Nakashima, S. *J. Am. Chem. Soc.* **1985**, *107*, 7996.

[5] Morrison, W. H., Jr.; Hendrickson, D. N. *Inorg. Chem.* **1975**, *14*, 2331.

[6] Iijima, S.; Saida, R.; Motoyama, I.; Sano, H. *Bull. Chem. Soc. Jpn.* **1981**, *54*, 1375.

0002-7863/86/1508-0963$01.50/0